Hybrid Near-Optimal Aeroassisted Orbit Transfer Plane Change Trajectories

Gregory A. Dukeman* and Anthony J. Calise**

Abstract

In this paper, a hybrid methodology is used to determine optimal open loop controls for the atmospheric portion of the aeroassisted plane change problem. The method is hybrid in the sense that it combines the features of numerical collocation with the analytically tractable portions of the problem which result when the two-point boundary value problem is cast in the form of a regular perturbation problem. Various levels of approximation are introduced by eliminating particular collocation parameters and their effect upon problem complexity and required number of nodes is discussed. The results include plane changes of 10, 20, and 30 degrees for a given vehicle.

Introduction

This paper is an extension of [5]. It is well-known that aeroassisted orbit changes require significantly less fuel than all-propulsive maneuvers. In particular, the orbital plane change is very costly in terms of fuel. In order to realize the potential savings afforded by aeroassist it is important to develop computationally efficient and reliable algorithms suitable for computing near-optimal trajectories in real-time. Exact solutions are typically too computationally intensive to compute onboard. On the other hand, approximate analytical solutions often result in too great of a loss in optimality or generality to be of any use.

The present method combines the desirable features of both analytical methods and numerical methods. The two-point boundary value problem resulting from the optimal control problem is first cast as a regular perturbation problem by artificially introducing small parameters and adjustable collocation parameters into the state/costate system. The trajectory is then divided into a finite number of intervals wherein the solution is approximated by the analytical zeroth order solution of the regular perturbation problem.

Recently, numerous approximate methods have been used to compute near-optimal controls for aeroassisted transfer [1-3]. These approximations have assumed that Keplerian effects are small. The Keplerian effects are treated by assuming that Loh's term

---

* Aerospace Engineer, Flight Mechanics Branch, Marshall Space Flight Center, Huntsville, Alabama.

** Professor, School of Aerospace Engineering, Georgia Institute of Technology, Atlanta, Georgia. Fellow AIAA.

is constant or piecewise constant [2]. Alternatively, the problem can be treated as a regular perturbation of the control solution [1]. In [4] it is shown that the problem is a singularly perturbed problem and that the Keplerian effects can be treated by matching a zero-order outer solution with the zero-order solution in [1] .

Equations of Motion

The equations of motion for a particle of mass m about a spherical non rotating planet are

$$\begin{aligned}
\dot{r} &= V\sin\gamma \\
\dot{V} &= -\frac{D}{m} - g\sin\gamma \\
\dot{\gamma} &= \frac{L\cos\mu}{mV} - \left(\frac{g}{V} - \frac{V}{r}\right)\cos\gamma \\
\dot{\psi} &= \frac{L\sin\mu}{mV\cos\gamma} - \frac{V}{r}\cos\gamma\cos\psi\tan\phi \\
\dot{\phi} &= \frac{V\cos\gamma\sin\psi}{r} \\
\dot{\theta} &= \frac{V\cos\gamma\cos\psi}{r\cos\phi}
\end{aligned} \tag{1}$$

where the dot denotes derivatives with respect to the independent variable t, r is the distance from the center of mass of the planet to the point mass, V is the speed, γ is the flight path angle, ψ is the heading angle, ϕ is the cross range angle, θ is the downrange angle, μ is the bank angle, and g is the local gravitational acceleration in an inverse square field. The atmospheric density ρ is modeled by

$$\rho = \rho_s e^{-\left(\frac{r-r_s}{\beta}\right)} \tag{2}$$

where ρ_s is a reference density, r_s is the reference radius, and β is the scale height. The aerodynamic forces are given by

$$L = \frac{1}{2}\rho V^2 S C_L$$
$$D = \frac{1}{2}\rho V^2 S C_D \qquad (3)$$
$$C_D = C_{D_0} + K C_L^2$$

where L is the lift force, D is the drag force, C_L is the lift coefficient, C_D is the drag coefficient, C_{D_0} is the drag coefficient at zero lift, S is the aerodynamic reference area, and K is a constant.

To facilitate analysis, these equations are modified through several transformations and assumptions as in [1]. First, introduce non-dimensional variables defined by

$$w = \frac{C_L^* \rho S \beta}{2m} \qquad \lambda = \frac{C_L}{C_L^*}$$
$$v = \ln\left(\frac{V^2}{gr}\right) \qquad \delta = \lambda \cos\mu \qquad (4)$$
$$E^* = \frac{C_L^*}{C_D^*} \qquad \sigma = \lambda \sin\mu$$

where w and v are the non dimensional variables related to altitude and velocity, respectively, and λ is the normalized lift coefficient. E^* denotes the maximum lift-to-drag ratio, and C_L^* and C_D^* are given by

$$C_D^* = 2C_{D_0} = 2KC_L^{*2} \qquad (5)$$

The new controls σ and δ are the local vertical and local horizontal components of normalized lift.

Under various assumptions made in [2] and [6] cross range and downrange become ignorable coordinates so that the resulting equations of motion are :

$$
\begin{aligned}
w' &= -\gamma \\
v' &= -\frac{\left(1+\sigma^2+\delta^2\right)}{E^*} - \varepsilon\left[\frac{r_s(2e^{-v}-1)\gamma}{rw}\right] \\
\gamma' &= \delta + \varepsilon\left[\frac{r_s(1-e^{-v})}{rw}\right] \\
\psi' &= \sigma
\end{aligned}
\tag{6}
$$

where the prime denotes derivatives with respect to a new independent variable z. The change in inclination is approximated by the change in heading.

Optimal Control Formulation

The associated optimal control problem is to minimize the energy loss, or equivalently, to maximize the final velocity subject to the equations of motion, specified initial conditions, and specified terminal values of altitude, flight path angle, and heading. The Hamiltonian H for this problem is given by

$$
H = \lambda_\psi \sigma - \lambda_w \gamma + \lambda_\gamma\left[\delta + \varepsilon\left(\frac{r_s(1-e^{-v})}{rw}\right)\right] - \lambda_v\left[\frac{(1+\sigma^2+\delta^2)}{E^*} + \varepsilon\left(\frac{r_s(2e^{-v}-1)\gamma}{rw}\right)\right] \tag{7}
$$

The optimality conditions $H_\sigma = 0$, $H_\delta = 0$,can be solved for the controls in terms of the costates

$$
\delta = \frac{E^*\lambda_\gamma}{2\lambda_v} \qquad \sigma = \frac{E^*\lambda_\psi}{2\lambda_v} \tag{8}
$$

Hybrid Solution: Zero-Order Approximation with Collocation

As in [5], we divide the trajectory into N intervals, introduce a "small" parameter ε, introduce collocation parameters p's and q's and write the state/costate system for interval j as:

$$
\begin{aligned}
w' &= -\gamma \\
v' &= -\frac{\left(1+\sigma^2+\delta^2\right)}{E^*} + p_{v_j} - \varepsilon\left[\frac{\beta(2e^{-v}-1)\gamma}{rw} - p_{v_j}\right] \\
\gamma' &= \delta + p_{\gamma_j} + \varepsilon\left[\frac{\beta(1-e^{-v})}{rw} - p_{\gamma_j}\right] \\
\psi' &= \sigma \\
\lambda_w' &= q_{w_j} + \varepsilon\left(-\frac{\partial H}{\partial w} - q_{w_j}\right) \\
\lambda_v' &= q_{v_j} + \varepsilon\left(-\frac{\partial H}{\partial v} - q_{v_j}\right) \\
\lambda_\gamma' &= \lambda_w + q_{\gamma_j} + \varepsilon\left(-\frac{\partial H}{\partial \gamma} - \lambda_w - q_{\gamma_j}\right) \\
\lambda_\psi' &= 0
\end{aligned}
\tag{9}
$$

for all $z \in [z_{j-1}, z_j]$, and H is the Hamiltonian. Note that for the case $\varepsilon = 0$ the system of differential equations (9) has an analytical solution (see the Appendix) which allows any of the states or costates to be computed in any given interval as functions of the collocation parameters for that interval, the quantity $z - z_{j-1}$, and the state/costate values at the beginning of the interval. This analytic solution provides the interpolating functions in the collocation method. The terms in (9) that are multiplied by ε serve as "defect" equations, i.e., the p's and q's are determined such that these terms are zero at the midpoint of each interval. In this way, the p's and q's in the interpolating functions account for the parts of the state/costate system that are not analytically tractable. Note that if ε is set to a nominal value of unity, then the original state/costate system is recovered. Therefore, as the number of elements N becomes large, the hybrid solution approaches the exact solution.

The optimal control problem has been reduced to a problem in nonlinear equation solving. Five defect equations exist per interval for computing the five collocation parameters per interval and the unknown initial costates and final time can be solved for by enforcing the specified and natural boundary conditions that arise from optimal control theory. Instead of solving for unknown final time, the trajectory can be divided into intervals in the heading angle, the final value of which is specified. In all, there are 5N + 4 equations and 5N + 4 unknowns. In the next section, numerical results are shown which compare solutions obtained using three different sets of interpolating functions: the first set is obtained from neglecting the analytically intractable part of the nu dot and lambda-nu dot equations thus eliminating the p_v and q_v collocation parameters in the interpolation

functions. Similarly, the second and third sets of interpolating functions are obtained from neglecting the analytically intractable parts of the nu dot and lambda-nu dot equations respectively. The first set results in a constant lambda-nu whereas the second set results in a piecewise linear lambda-nu history; thus reference will be made later to the constant lambda-nu and linear lambda-nu formulations respectively. The third set will be referred to as the precise nu formulation.

Numerical Results

The methodology described above is used here to compute near-optimal open loop controls for the vehicle described in [3] while executing a plane change maneuver. The physical constants are K=1.4, $C_{D_0} = 0.032, S = 11.69\text{m}^2$, and $m = 4898.7$ kg. The modeling parameters are the scale height $\beta = 8251.585$ m, reference radius $r_s = 6.433375\text{E}6$ m, reference density $\rho_s = 5.6075\text{E} - 4 \text{ kg/m}^3$, and the gravitational constant $\overline{\mu} = 3.98603\text{E}14 \text{ m}^3/\text{s}^2$. Initial conditions are altitude H_i = 60 km, V_i = 7850.88 m/s, $\gamma_i = -1.346$ deg, and $\psi_i = 0$ deg. Final conditions are H_f = 60 km, $\gamma_f = 1.0$ deg, and $\psi_f = 20$ deg. The numerical results presented here are for the three different formulations (i.e., three different sets of interpolating functions) discussed above with varying numbers of nodes and varying plane change angles.

Figures 1 through 5 show state and control histories corresponding to trajectories generated using eight equally spaced nodes. Trajectories corresponding to plane change angles of 10, 20 and 30 degrees were computed. The only noticeable differences between the three trajectories for a given plane change is in the altitude histories. The trajectory resulting from the linear lambda-nu formulation penetrates slightly deeper into the atmosphere than either the constant lambda-nu formulation or the precise nu formulation. The precise nu formulation trajectories are indistinguishable from the constant lambda-nu formulation trajectories.

Exit speeds for various combinations of formulation, plane change and number of elements are presented in Tables 1 and 2. For N = 8 elements and a plane change of 20 degrees, the exit speed corresponding to the constant lambda-nu trajectory is 6737 m/s compared with 6738 m/s for the piece wise linear lambda-nu trajectory. The difference in performance between these two formulations is very small and certainly does not justify the relatively complex interpolating functions for the case of linear lambda-nu.

Figure 6 compares altitude histories generated using different numbers of nodes. The closeness of these histories suggests that 6 equally spaced elements provide sufficient accuracy for trajectory generation. An attempt was made to use just four equally spaced elements but the resulting trajectory was physically unrealistic, e.g., the speed increased monotonically in the atmosphere. This is due to the nature of the methodology used here. The differential equations are only enforced at the midpoints of the elements so that if an

insufficient number of elements is used physically unrealistic trajectories result. In [5] nonuniform spacing of the nodes was used to generate accurate trajectories with only four elements.

Discussion

The linear lambda-nu formulation does not significantly improve the performance or accuracy of the generated trajectories. Thus, it is apparently unnecessary to use the complicated interpolating functions that result from the linear lambda-nu formulation. These functions contain logarithms which make the nonlinear problem harder to solve numerically. For the constant lambda-nu formulation (as well as the precise nu formulation), the interpolating functions degenerate into simple polynomials [5].

The precise nu formulation trajectories are virtually identical to the constant lambda-nu formulation trajectories. However, there is a noticeable difference in the exit speeds which may or may not be acceptable depending upon the application. If one were to use the constant lambda-nu formulation in the form of a closed loop guidance scheme, the difference in exit speed of the guided trajectories may very well be negligible as compared to using the precise nu formulation as a closed loop guidance scheme. The controls histories represented by bank angle and normalized lift coefficient for a typical trajectory differ by no more than 0.1 deg and 0.005 respectively. Regarding complexity, the constant lambda-nu formulation involves 3N+4 (N is the number of elements used) problem variables as compared to 4N+4 problem variables for the precise nu formulation. For N = 6, this gives 22 and 28 problem variables respectively. The interpolating functions are identical except for an additional linear term in the precise nu formulation.

Conclusions

Zero-order analytic solutions to various levels of approximation of the aeroassisted optimal plane change problem have been obtained for use as interpolating functions in a collocation method. The simplest formulation, whrerein a constant lambda-nu is assumed, is shown to provide sufficient accuracy in determining near-optimal open-loop controls and by nature of its simplicity has potential for use as a closed loop guidance scheme. The hybrid methodology used here to develop intelligent interpolating functions allows accurate trajectory generation with only a small number of equally spaced nodes in the collocation

method. Further work could be done using the hybrid methodology to solve the more realistic problems of heating or load constrained aeroassisted plane change maneuvers.

References

1. Speyer, J.L., and Crues, E.Z., "Approximate Atmospheric Guidance Law for Aeroassisted Plane Change Maneuvers," Journal of Guidance, Control, and Dynamics, Vol. 13, No. 5, 1990, pp.792-802.

2. Hull, D.G., Giltner, J.M., Speyer, J.L., and Mapar, J., "Minimum Energy-Loss Guidance for Aeroassisted Orbital Plane Change," Journal of Guidance, Control, and Dynamics, Vol. 8, No.4, 1985, pp.487-493.

3. Hull, D.G., and Speyer, J.L., "Optimal Re-entry and Plane Change Trajectories," Journal of the Astronautical Sciences, Vol.XXX, 1982, pp. 117-130.

4. Calise, A.J., and Melamed, N., "Optimal Guidance of Aero-assisted Transfer Vehicles Based on Matched Asymptotic Expansions," Proceedings of the AIAA Guidance, Navigation, and Control Conference, Vol. 2, AIAA, Washington, DC., 1991, pp.1048-1058.

5. McFarland, M., Calise, A., "A Hybrid Approach to Near-Optimal Atmospheric Guidance for Aeroassisted Orbit Transfer Maneuvers," AIAA Guidance, Navigation and Control Conf., Paper No. 93-3858, Monterey, CA, Aug 9-11, 1993, pp 1423-1430.

6. Mease, K.D., Lee, J.Y., and Vinh, N.X., "Orbital Change During Hypersonic Aerocruise," Journal of the Astronautical Sciences, Vol. 36, Nos. 1/2, 1988, pp. 103-137.

Figures (In the legends F1_N8 denotes formulation 1, 8 elements. Formulation 1 is the constant lambda-nu formulation, formulation 2 is the linear lambda-nu formulation, formulation 3 is the precise nu formulation)

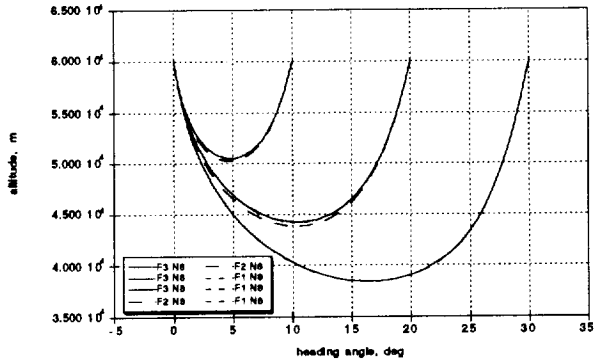

Figure 1: altitude vs heading angle

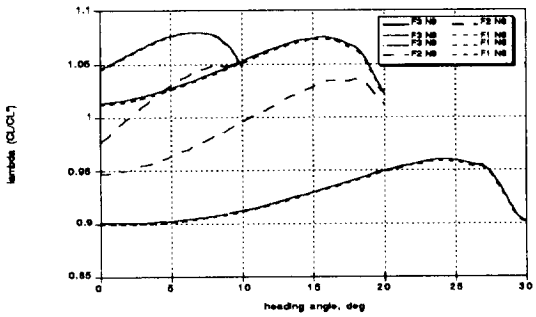

Figure 4: normalized lift coefficient vs heading angle

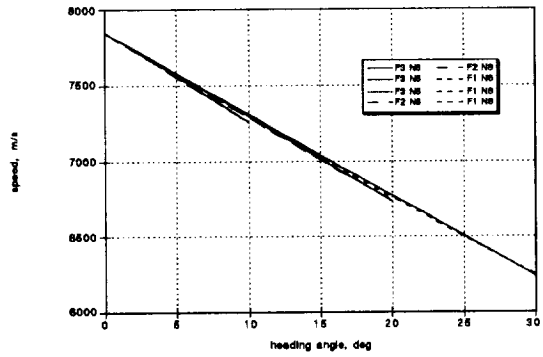

Figure 2: speed vs heading angle

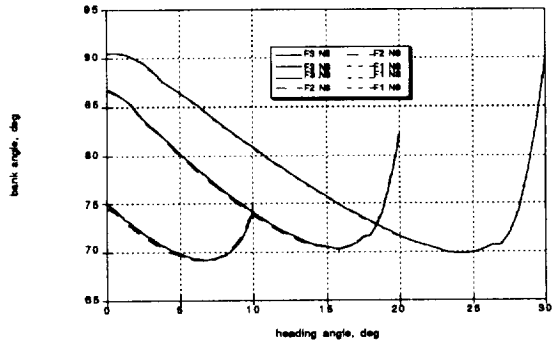

Figure 5: bank angle vs heading angle

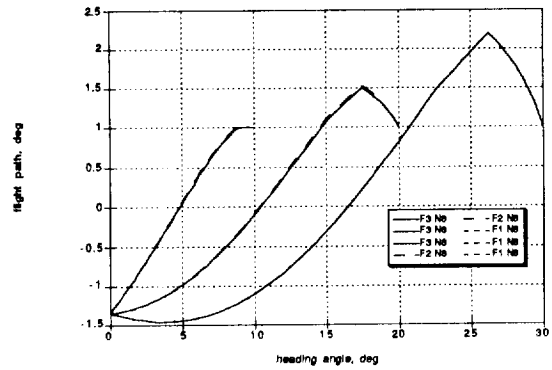

Figure 3: flight path vs heading angle

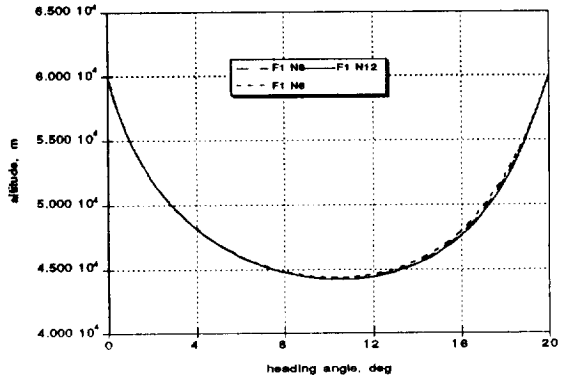

Figure 6: altitude vs heading for varying numbers of elements

Table 1. Exit Speeds for varying formulation and plane change angles.

plane change, deg	constant lambda-nu formulation exit speed, m/s	linear lambda-nu formulation exit speed, m/s	precise nu formulation, exit speed, m/s
10	7259.4	7260.1	7258.2
20	6737.0	6738.0	6733.2
30	6244.7	not calculated	6236.1

Table 2. Exit speeds for varying numbers of elements. Constant lambda-nu formulation, 20 degree plane change

number of elements	exit speed, m/s
6	6738.2
8	6737.0
12	6736.7

Appendix

The hybrid formulation of (9) gives rise to the following nonlinear interpolating functions.

$$\lambda_{\psi}(z) = \lambda_{\psi_{j-1}}$$
$$\lambda_{w}(z) = q_{w_j}\Delta z + \lambda_{w_{j-1}}$$

$$\lambda_{v}(z) = q_{v_j}\Delta z + \lambda_{v_{j-1}}$$
$$\lambda_{\gamma}(z) = \frac{q_{w_j}}{2}(\Delta z)^2 + \left(\lambda_{w_{j-1}} + q_{\gamma_j}\right)\Delta z + \lambda_{\gamma_{j-1}}$$

$$\psi(z) = \frac{E^*\lambda_{\psi_{j-1}}}{2q_{v_j}}\left[\ln(-q_{v_j}\Delta z - \lambda_{v_{j-1}}) - \ln(-\lambda_{v_{j-1}})\right]$$

$$\gamma(z) = \frac{q_w E^*}{8q_{v_j}}(\Delta z)^2 + \left[p_{\gamma} + \frac{E^*\left(2q_{v_j}q_{\gamma_j} + 2q_{v_j}\lambda_{w_{j-1}} - \lambda_{v_{j-1}}q_{w_j}\right)}{4q_{v_j}^2}\right]\Delta z +$$

$$\frac{E^*}{4q_{v_j}^3}\left[2q_{v_j}^2\lambda_{\gamma_{j-1}} - 2q_{v_j}\lambda_{v_{j-1}}\lambda_{w_{j-1}} - 2\lambda_{v_{j-1}}q_{v_j}q_{\gamma_j} + \lambda_{v_{j-1}}^2 q_w\right]\left[\ln(-q_{v_j}\Delta z - \lambda_{v_{j-1}}) - \ln(-\lambda_{v_{j-1}})\right] + \gamma_{j-1}$$

$$w(z) = -\frac{q_{w_j}E^*}{24q_{v_j}}(\Delta z)^3 + \left[-\tfrac{1}{2}p_{\gamma_j} - \frac{E^*\left(q_{v_j}q_{\gamma_j} + q_{v_j}\lambda_{w_{j-1}} - \tfrac{1}{2}\lambda_{v_{j-1}}q_{w_j}\right)}{4q_{v_j}^2}\right]\Delta z^2 +$$

$$\left\{\frac{E^*A}{4q_v^3}\left[1 - \ln\left(-q_{v_j}\Delta z - \lambda_{v_{j-1}}\right) + \ln\left(-\lambda_{v_{j-1}}\right)\right] - \gamma_{j-1}\right\}\Delta z +$$

$$\frac{E^*\lambda_{v_{j-1}}A}{4q_v^4}\left[1 - \ln(-q_{v_j}\Delta z - \lambda_{v_{j-1}}) + \ln(-\lambda_{v_{j-1}})\right] + w_{j-1}$$

$$v(z) = B(z) - B(z_{j-1}) + v_{j-1}$$

where $j = 1\ldots N$, $\Delta z = (z - z_{j-1})$, and $z \in \left[z_{j-1}, z_j\right]$.

A is given by:

$$A = 2q_{v_j}^2\lambda_{\gamma_{j-1}} - 2q_{v_j}\lambda_{v_{j-1}}\lambda_{w_{j-1}} - 2\lambda_{v_{j-1}}q_{v_j}q_{\gamma_j} + \lambda_{v_{j-1}}^2 q_w$$

and $B(z)$ is given by:

$$B(z) = -\frac{1}{E^*}\left(\Delta z - \frac{E^{*2}\lambda^2_{w_{j-1}}}{\lambda_v(z)q_{v_j}} + \frac{E^{*2}}{4}\left(\frac{1}{4q^4_{v_j}}\begin{pmatrix} \frac{1}{3}q^2_{w_{j-1}}q^2_{v_{j-1}}(\Delta z)^3 + 2q_{w_{j-1}}q^2_{v_{j-1}}q_{\gamma_{j-1}}(\Delta z)^2 \\ +2q_{w_{j-1}}q^2_{v_{j-1}}\lambda_{w_{j-1}}(\Delta z)^2 + 4q_{w_{j-1}}q^2_{v_{j-1}}\lambda_{\gamma_{j-1}}\Delta z \\ +4q^2_{v_{j-1}}q^2_{\gamma_{j-1}}\Delta z + 4q^2_{v_{j-1}}\lambda^2_{w_{j-1}}\Delta z \\ +8q^2_{v_{j-1}}q_{\gamma_{j-1}}\lambda_{w_{j-1}}\Delta z - q^2_{w_{j-1}}q_{v_{j-1}}\lambda_{v_{j-1}}(\Delta z)^2 \\ -8q_{w_{j-1}}q_{v_{j-1}}q_{\gamma_{j-1}}\lambda_{v_{j-1}}\Delta z - 8q_{w_{j-1}}q_{v_{j-1}}\lambda_{w_{j-1}}\lambda_{v_{j-1}}\Delta z \\ +3q^2_{w_{j-1}}\lambda^2_{v_{j-1}}\Delta z \end{pmatrix} - \right.\right.$$

$$\left.\left. \frac{1}{4q^8_{v_j}\lambda_v(z)}\begin{pmatrix} +4q^7_{v_{j-1}}\lambda^2_{\gamma_{j-1}} + 4q^5_{v_{j-1}}q^2_{w_{j-1}}\lambda^2_{v_{j-1}}\lambda_{\gamma_{j-1}} \\ +4q^5_{v_{j-1}}\lambda^2_{w_{j-1}}\lambda^2_{v_{j-1}} + 8q^5_{v_{j-1}}q_{\gamma_{j-1}}\lambda_{w_{j-1}}\lambda^2_{v_{j-1}} \\ +4q^5_{v_{j-1}}q^2_{\gamma_{j-1}}\lambda^2_{v_{j-1}} + q^2_{w_{j-1}}q^3_{v_{j-1}}q^2_{\gamma_{j-1}}\lambda^4_{v_{j-1}} \\ -4q_{w_{j-1}}q^4_{v_{j-1}}q^2_{\gamma_{j-1}}\lambda_{w_{j-1}}\lambda^3_{v_{j-1}} - 4q_{w_{j-1}}q^4_{v_{j-1}}q_{\gamma_{j-1}}\lambda^3_{v_{j-1}} \\ -8q^6_{v_{j-1}}\lambda_{w_{j-1}}\lambda_{v_{j-1}}\lambda_{\gamma_{j-1}} - 8q^6_{v_{j-1}}q_{\gamma_{j-1}}\lambda_{v_{j-1}}\lambda_{\gamma_{j-1}} \end{pmatrix} + \right.\right.$$

$$\left.\left. \frac{\ln(-\lambda_v(z))}{4q^8_{v_j}}\begin{pmatrix} 8q^6_{v_{j-1}}\lambda_{w_{j-1}}\lambda_{\gamma_{j-1}} + 8q^6_{v_{j-1}}q_{\gamma_{j-1}}\lambda_{\gamma_{j-1}} \\ +12q_{w_{j-1}}q^4_{v_{j-1}}\lambda_{w_{j-1}}\lambda^2_{v_{j-1}} + 12q_{w_{j-1}}q^4_{v_{j-1}}q_{\gamma_j}\lambda^2_{v_{j-1}} \\ -4q^2_{w_{j-1}}q^3_{v_{j-1}}\lambda^3_{v_{j-1}} - 8q_{w_{j-1}}q^5_{v_{j-1}}\lambda_{v_{j-1}}\lambda_{\gamma_{j-1}} \\ -8q^5_{v_{j-1}}\lambda^2_{w_{j-1}}\lambda_{v_{j-1}} - 16q^5_{v_{j-1}}q_{\gamma_{j-1}}\lambda_{w_{j-1}}\lambda_{v_{j-1}} \\ -8q^5_{v_{j-1}}q^2_{\gamma_{j-1}}\lambda_{v_{j-1}} \end{pmatrix} \right.\right.$$

$$\left.\left. \right)\right)$$

$$+ p_{v_j}\Delta z$$